Deep-Sea Research I 97 (2015) 1–9

Contents lists available at ScienceDirect

Deep-Sea Research I

journal homepage: www.elsevier.com/locate/dsri

Instruments and Methods

Design, construction, and operation of an actively controlled deep-sea CO_2 enrichment experiment using a cabled observatory system

William J. Kirkwood, Peter M. Walz, Edward T. Peltzer, James P. Barry, Robert A. Herlien, Kent L. Headley, Chad Kecy, George I. Matsumoto, Thom Maughan, Thomas C. O'Reilly, Karen A. Salamy, Farley Shane, Peter G. Brewer *

Monterey Bay Aquarium Research Institute (MBARI), 7700 Sandholdt Road, Moss Landing, CA 95039-9644, USA

ARTICLE INFO

Article history:
Received 5 May 2014
Received in revised form
7 November 2014
Accepted 11 November 2014
Available online 25 November 2014

Keywords:
MARS cable
CO_2 enrichment
Ocean acidification

ABSTRACT

We describe the design, testing, and performance of an actively controlled deep-sea Free Ocean CO_2 Enrichment (dp-FOCE) system for the execution of seafloor experiments relating to the impacts of ocean acidification on natural ecosystems. We used the 880 m deep MARS (Monterey Accelerated Research System) cable site offshore Monterey Bay, California for this work, but the Free Ocean CO_2 Enrichment (FOCE) system concept is designed to be scalable and can be modified to be used in a wide variety of ocean depths and locations. The main frame is based on a flume design with active thruster control of flow and a central experimental chamber. The unit was allowed to free fall to the seafloor and connected to the cable node by remotely operated vehicle (ROV) manipulation. For operation at depth we designed a liquid CO_2 containment reservoir which provided the CO_2 enriched working fluid as ambient seawater was drawn through the reservoir beneath the more buoyant liquid CO_2. Our design allowed for the significant lag time associated with the hydration of the dissolved CO_2 molecule, resulting in an e-folding time, τ, of 97 s between fluid injection and pH sensing at the mean local $T=4.31\pm0.14$ °C and pH_T of 7.625 ± 0.011. The system maintained a pH offset of ~0.4 pH units compared to the surrounding ocean for a period of ~1 month. The unit allows for the emplacement of deep-sea animals for testing. We describe the components and software used for system operation and show examples of each. The demonstrated ability for active control of experimental systems opens new possibilities for deep-sea biogeochemical perturbation experiments of several kinds and our developments in open source control systems software and hardware described here are applicable to this end.

1. Introduction

With the recent introduction of cabled observatory systems (Favali and Beranzoli, 2006; Massion and Raybould, 2006; Favali et al., 2010) new opportunities for deep-sea experimental science have arisen. While many of the instruments that have been deployed on such cables can report in real-time through their power and optical fiber connectivity they are still in a sense passive instruments that simply record the events of the natural world around them.

We describe here the creation of an actively controlled deep-sea experimental system for investigation of the impacts of elevated oceanic CO_2 levels on seafloor marine ecosystems from concept through design, testing, and construction into full operation. The system may also be adapted to experiments controlling dissolved O_2 levels or for a combination of CO_2 and O_2 perturbation experiments. Although the system described here was developed for deep-sea operation, the intent has been to understand the fundamental physical and chemical principles involved in order to produce a fully scalable system with sufficient design flexibility so that other deep and/or shallow water systems of varying dimensions can be adapted from it. This technology transfer process is already occurring at several other Free Ocean CO_2 Enrichment (FOCE) sites (Kline et al., 2012; Gattuso et al., 2014).

The impetus for creation of a pH controlled experimental system may be traced to concerns that arose when small-scale direct deep-ocean CO_2 disposal experiments were carried out at a depth of 3600 m (Brewer et al., 1999). These efforts were driven by the recommendations of a US President's Council of Advisors on Science and Technology report (PCAST (President's Council of Advisors on Science and Technology), 1997) that, following an idea first

* Corresponding author. Tel.: +1 831 775 1706; fax: +1 831 775 1620.
E-mail address: brpe@mbari.org (P.G. Brewer).

http://dx.doi.org/10.1016/j.dsr.2014.11.005
0967-0637/

suggested by Marchetti (1977), advocated direct disposal of captured fossil fuel CO_2 in the deep ocean where it was presumed a stable solid hydrate would form. The images from that deep-sea experiment of a fish swimming by a beaker of overflowing liquid CO_2, driven by formation of solid CO_2 hydrate, stimulated long-latent awareness of both the true scale of future fossil fuel CO_2 emissions and the difficulty of dealing with this (Cicerone et al., 2004; Shirayama and Kogure, 2004; IPCC, 2005). Until that time the beneficial role of large scale ocean absorption of fossil fuel CO_2 from the atmosphere was the dominant focus of scientists, although in retrospect the warning signs of the forced changes in ocean chemistry were present for many decades (Brewer, 2013). Simultaneously with the interest in direct deep-ocean CO_2 disposal, large scale under-sea geologic sequestration of CO_2 produced from offshore oil and gas fields began and questions over the impact of any future seafloor CO_2 leakage arose (Widdicombe et al., 2013).

Early experiments on biological impacts of artificially elevated CO_2 levels in the deep sea (3600 m) were reported by Tamburri et al. (2000) and by Barry et al. (2004, 2005). These were carried out with single pools of liquid CO_2 as the CO_2 source. The physical properties of liquid CO_2 are such that at depths below about 2600–2800 m (depending upon the in situ temperature) it is denser than sea water and thus gravitationally stable on the seafloor (Brewer et al., 1999). This allows experimental emplacement of an open pool of liquid CO_2 that creates a dense plume of low pH water as the CO_2 dissolves into the surrounding seawater. When these first experiments were conducted to assess the impact of low pH/high CO_2 seawater on local marine life it was quickly realized that the effect of the local tidal ellipse was to create a highly variable diurnal ΔpH signal which greatly exceeded the natural background variations.

These experiments, while accurately depicting the locally varying small-scale pH field around a liquid CO_2 disposal event, did not provide a useful way of assessing long-term marine life impacts of a future high CO_2 ocean although valuable short term impact studies emerged (Thistle et al., 2006, 2007); animals at a specific site were exposed to a low pH/high CO_2 plume for only a short time twice a day. To be useful for long-term assessment of biological and organismal impacts of ocean acidification some greater degree of control over CO_2 enrichment and flow rate within a specified volume is required so that a reasonably constant pH offset above the varying natural background can be maintained.

We realized that lessons could be learned from the global series of FACE (Free Air CO_2 Enrichment) terrestrial ecosystem experiments (DeLucia et al., 1999; Shaw et al., 2002). That effort demonstrated that experiments within greenhouses showing strong stimulation of plant growth from elevated atmospheric CO_2 levels might not apply to the real, more complex, open world of climate change. The net result from a very large number of these FACE field experiments was that natural land ecosystems would benefit little, if at all, from elevated CO_2 levels (Long et al., 2006).

Similarly, aquaria pH perturbation experiments might not adequately represent impacts on complex ecosystems and careful in situ studies may show problems, or resilience and abilities to compensate in some species. We will not know unless competent experiments at a wide variety of sites can be carried out and we can advance beyond single species aquarium studies; here we describe progress in creating such field experimental systems.

2. Initial studies

2.1. First attempts at a CO_2 enrichment control system

Three principles guided the design and operation of the FOCE experimental system. (1) The system needs to be "open to the ocean" in such a way that natural variations in S, T, P, O_2, TAlk and food supply are not altered. Unlike experiments in aquaria where these parameters are often held constant, FOCE experiments should reflect natural variations and diurnal to seasonal cycles as much as possible. (2) The system is intended to be a total CO_2 enrichment experiment not a pH experiment. TCO_2 levels are increased without changing the alkalinity in order to achieve pCO_2 levels predicted for the next century through the addition of dissolved CO_2, not by the addition of bicarbonate or strong mineral acids. (3) The resulting change in pH is used to monitor the change in TCO_2 and pCO_2 in order to provide real-time feedback and control of the CO_2 addition.

On land the tactic has been to encircle an area of vegetation with a ring of controlled CO_2 gas emitters programmed to release only from the upwind sector of the ring. It is clear that very different experimental constraints apply in the ocean. The physical forces on the apparatus are larger, and the experimental set-up is more challenging whether by scuba divers or by remotely operated vehicles (ROVs). Most importantly, CO_2 in sea water has a complex chemistry with significant reaction rate kinetics (Zeebe and Wolf-Gladrow, 2001) that greatly impacts the ability to sense and thus control a plume of CO_2 enriched sea water (Brewer et al., 2005). In our Supporting Information, we describe the early experiment development which began with a simple ring structure system test. This quickly led to the need for providing a delay time between addition of the CO_2 rich working fluid and the observation chamber to allow time for the hydration of the aqueous CO_2 molecule to proceed and thus provide the desired pH perturbation.

2.2. Experimentally defining the chemical reaction rates and design implications

The essential chemical reaction rates for the hydration of CO_2 in sea water have been carefully observed in the laboratory (Johnson, 1982; Soli and Byrne, 2002). This information was gathered and incorporated into a rigorous theoretical treatment by Zeebe et al. (1999) and Zeebe and Wolf-Gladrow (2001). The end result is a series of equations where the relaxation time, τ, is dependent upon total CO_2 concentration, temperature, pressure, and the final pH of the system.

We have conducted the essential field measurements of these basic reaction rate equations developed from laboratory data in the deep waters of Monterey Bay. We used a closed cell pH perturbation technique first reported by Nakayama et al. (2005) in which we used a ROV (Fig. 1a) to carry and control a simple titration cell (Fig. 1b) to depth and followed the time course of the pH curve resulting from injection of various volumes of CO_2 saturated seawater (Fig. 1c and d). The pH data within the cell as a function of time obtained in situ was first converted into the concentration of OH^- and the best fit to the exponential decay curve was then found to determine the experimentally measured τ. These experiments are fairly quick to execute and within a single ROV dive we were able to make measurements over a span of temperature, pressure, pH and δCO_2 conditions.

The Zeebe and Wolf-Gladrow (2001) CO_2 kinetic model is based upon the interaction of the two competing reactions of CO_2 with water as a function of pH:

$$CO_2 + H_2O \underset{k_{-1}}{\overset{k_{+1}}{\rightleftharpoons}} HCO_3^- + H^+ \quad (1)$$

$$CO_2 + OH^- \underset{k_{-4}}{\overset{k_{+4}}{\rightleftharpoons}} HCO_3^- \quad (2)$$

the dissociation of bicarbonate ion and the dissociation of water:

$$HCO_3^- \rightleftharpoons CO_3^{2-} + H^+ \quad (3)$$

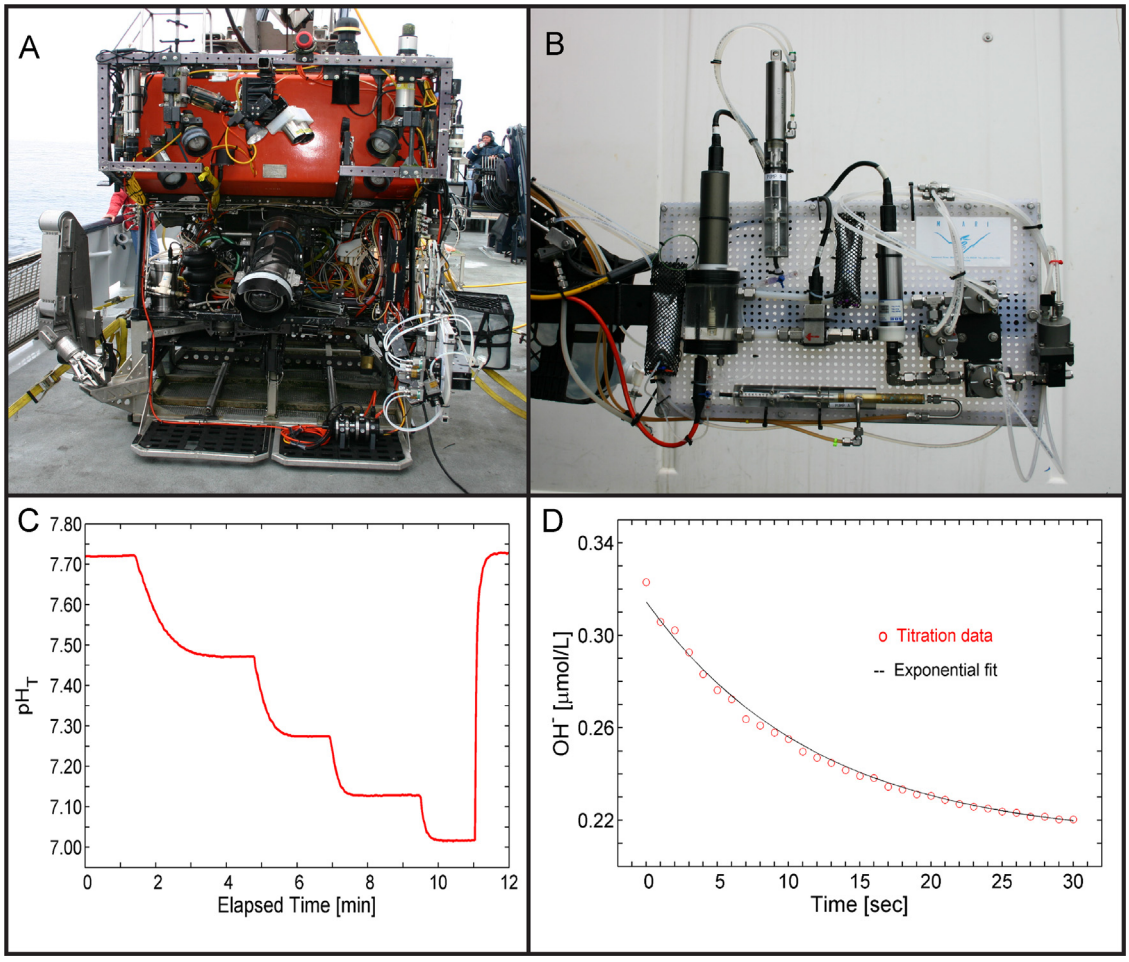

Fig. 1. (a) ROV Ventana sitting on the deck of R/V Point Lobos during final check-out procedure and ready to dive. The titration cell and CO_2–ESW cubitainer are visible on the ROV swing-arm located on the lower port-side of the ROV. (b) The titration cell installed on the ROV Ventana for field observation of the relaxation time of an injected pulse of CO_2 rich sea water at the depth of the experimental site. (c) Observed pH changes at depth from a series of injections of CO_2 saturated seawater as hydration of the CO_2 molecule occurs. (d) Observed change in OH^- ion concentration for one of these injections. From these data the time constant, τ, for the control of a deep-sea CO_2 enrichment experiment can be determined. The data are a close fit to the Zeebe and Wolf-Gladrow (2001) model predicted τ values (see Fig. 2).

$$H_2O \rightleftharpoons H^+ + OH^- \tag{4}$$

for which the following equilibrium constants are defined:

$$K_2 = [CO_3^{2-}][H^+]/[HCO_3^-] \tag{5}$$

$$K_W = [H^+][OH^-]. \tag{6}$$

Zeebe and Wolf-Gladrow (2001) then defined the following equations for the reaction rate following a perturbation in TCO_2 or pH in terms of τ, the relaxation time (also known as the e-folding time) for the approach to equilibrium:

$$\frac{d(\delta CO_2)}{dt} = -\frac{1}{\tau}\delta CO_2 \tag{7}$$

where

$$\frac{1}{\tau} = k_{+1} - k_{-1}(\partial_S b[H^+] + \partial_S h[HCO_3^-]) - k_{-4}\partial_S b + k_{+4}([OH^-] + \partial_S oh[CO_2]) \tag{8}$$

and

$$\partial_S b \equiv \frac{\partial[HCO_3^-]}{\partial[CO_2]} = -\frac{[H^+] + 2[CO_3^{2-}]/(1+\alpha)}{K_2 + [H^+] + [CO_3^{2-}]/(1+\alpha)} \tag{9}$$

$$\partial_S h \equiv \frac{\partial[H^+]}{\partial[CO_2]} = -\frac{\partial_S b + 2}{1+\alpha} \tag{10}$$

$$\partial_S oh \equiv \frac{\partial[OH^-]}{\partial[CO_2]} = \alpha\frac{\partial_S b + 2}{1+\alpha} \tag{11}$$

and

$$\alpha = K_W/([H^+])^2 \tag{12}$$

$$[CO_3^{2-}] = \sum CO_2/(1 + [H^+]/K_2 + ([H^+])^2/K_1/K_2) \tag{13}$$

In Fig. 2 we show the results of comparing our experimentally determined relaxation times with those calculated from the Zeebe–Wolf-Gladrow model for the same P, T and final pH and TCO_2 conditions. Based upon the success of these ROV based experiments, we used the Zeebe and Wolf-Gladrow (2001) model to predict the CO_2 reaction kinetics at the seafloor conditions of the FOCE experiment (Fig. 3).

2.3. Selection of a site

Installation of a real-time controllable deep sea experiment requires uninterrupted power and communications and we selected the MARS (Monterey Accelerated Research System) cable site (Massion and Raybould, 2006) in Monterey Bay as the location to begin our FOCE studies. The main node for this cable is located 30 km offshore at a depth of 880 m with an annual mean temperature of 4.31 ± 0.14 °C and a mean pH_T of 7.625 ± 0.011. From these data and with reference to the predicted rates of carbonate species equilibrium kinetics (Fig. 3)

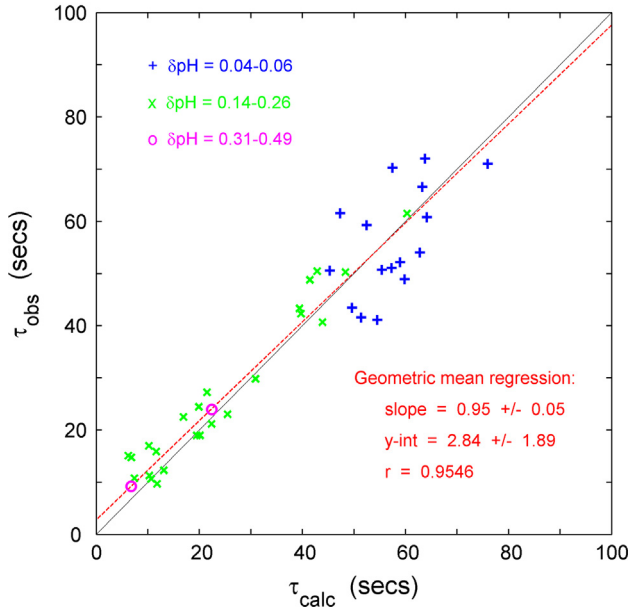

Fig. 2. Experimentally determined in situ values of τ versus those calculated from the Zeebe–Wolf-Gladrow model using the in situ salinity, temperature, pressure, total CO_2 and pH.

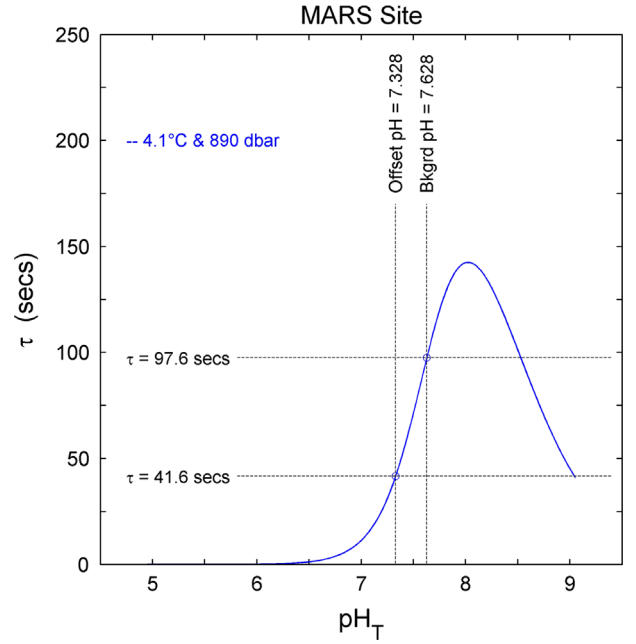

Fig. 3. The e-folding time predicted using the Zeebe and Wolf-Gladrow (2001) model for the MARS cabled site in Monterey Bay as a function of in situ salinity, temperature, pressure, pH and total CO_2 concentration. The slow reaction rates at low temperature are partially offset by the more acidic pH conditions in the lower O_2-higher CO_2 waters at depth.

we find that the e-folding time (τ) at this location is ~97 s at average background conditions but only 40 s within the FOCE experimental chamber with a reduced pH of 7.325 ($\Delta pH = -0.3$).

3. Materials and methods

3.1. Adoption of a basic flume design

The final FOCE design selected for the MARS site was a modified flume system (Fig. 4). This permits control of flow within the unit while maintaining open contact with the sediments. The design requires the addition of long wings connecting the CO_2 injection point to the control volume in the center of the unit. These serve as delay paths which allow the chemical reactions to approach equilibrium during the time interval between addition of the CO_2 enriched working fluid at the end of either wing, and arrival of the flow in the center control chamber. The CO_2 enriched sea water is denser than background sea water (Brewer and Bradshaw, 1975; Dunk et al., 2005) thus it is inevitable that small density differences will be created at the point of injection and the delay path also allows for significant mixing during transit so that density anomalies are minimized in the control chamber.

The scale of the demonstration unit was guided by the dimensions of the ROV system used for test deployments. It consisted of a box constructed of acrylic panels supported by fiberglass struts that also provided the mounting points for the required electronic housings and components. The dimensions of the central chamber were 2 m × 1 m × 50 cm. A hinged lid allowed the ROV to access the center control chamber for addition and removal of science experiments.

Controllable thrusters at each end of the central chamber provided flow to simulate the external environment and the tidal flow velocities characteristic of this deep sea location. Power and communication were provided by connecting the FOCE system to the main MARS cable node via an underwater mateable electro-optical cable and connector (ODI). An image of the assembled system in the fully deployed state is shown in Fig. 5 (right panel). For launch and recovery the side arms were folded up and latched together (Fig. 5, left panel). Blocks of syntactic foam were attached for suitable buoyancy and vertical stability during the free fall deployment of FOCE from the ocean surface. During deployment 90 kg of lead was added to make the flume 45 kg negatively buoyant to allow rapid sinking and minimal lateral drift from the launch point. Once deployed and on the sea-floor, the entire unit was picked up by the ROV and moved to the desired site close to the MARS power and communications node. At this point the latch was released and the side arms were fully opened (Fig. 5 right panel). For recovery the side arms were re-folded and latched, then removal of the 90 kg of lead resulted in 45 kg of positive buoyancy for rapid recovery by free ascent to the sea surface for ship recovery.

A dual valve system allowed the CO_2 enriched seawater to be delivered to either end of the FOCE frame. The electrically actuated valves were deployed in an oil-filled housing and were manually controlled via the FOCE GUI (see FOCE Flume Electronics and GUI in the Supporting Information). The basic plan of operation was to drive the water-flow inside the flume in the same direction as the exterior flow—both to avoid fighting the current and to exhaust the low pH seawater water down-stream from the experiment. The controllable thrusters modulated the velocity inside the flume to match the exterior velocity as much as possible.

3.2. Design of a CO_2 enriched sea water system

The enriched sea water (ESW) delivery system was based upon the system of Dunk et al. (2005) in which a contained volume of buoyant liquid CO_2 was allowed to slowly dissolve into a slow flow of sea water beneath it. The resultant highly CO_2 rich/low pH sea water is denser than the ambient seawater and sinks to the bottom of the container and is then drawn off to serve as the working fluid for the FOCE system. Under the temperature and pressure conditions at the site we are well within the CO_2 hydrate stability conditions and therefore hydrate formation could in theory provide significant flow blockage to our delivery lines. In practice, massive CO_2 hydrate formation did not occur although a hydrate skin formed at the liquid CO_2-sea water interface within the CO_2

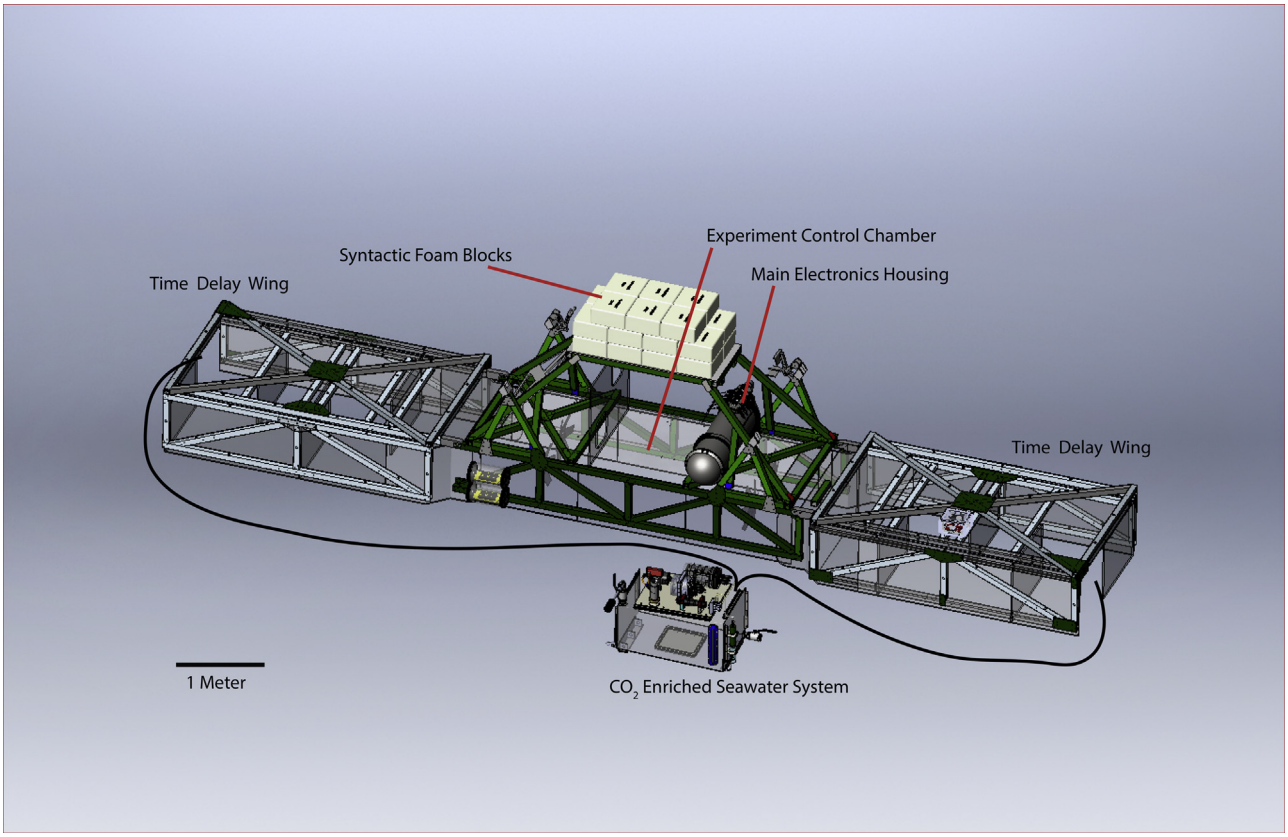

Fig. 4. Drawing of the assembled system in the deployed state with the folding time delay wings in the fully deployed condition. A more detailed drawing of the enriched sea water system is provided in the supporting materials.

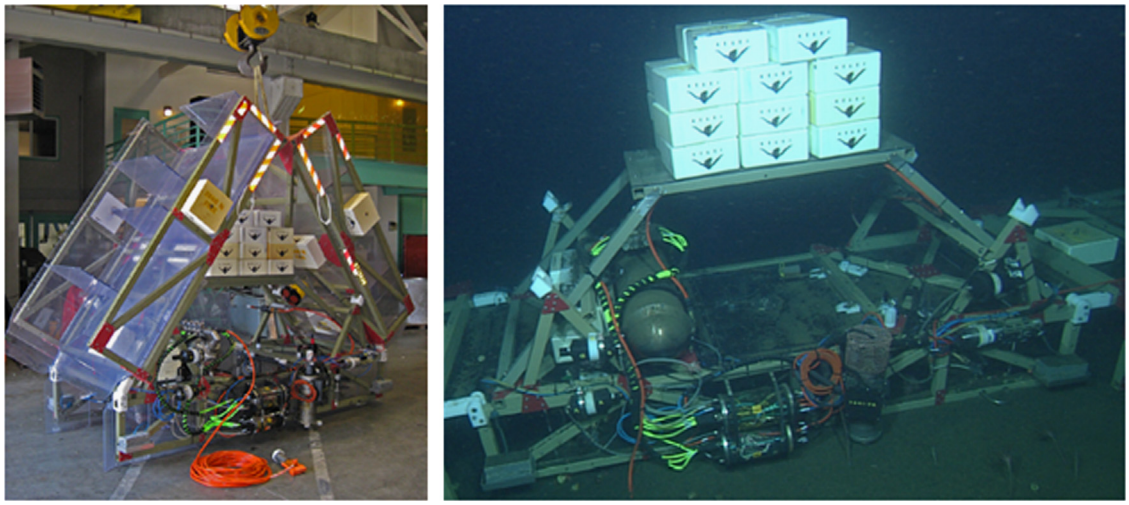

Fig. 5. Left panel: FOCE frame in the folded position prior to deployment. A lifting bail at the center also served to help latch the two wings together for deployment and recovery. This bail was also used by the ROV to move the frame into position near the MARS Cabled Observatory node. Right panel: Once in position, the ROV unlatched the two wings and carefully lowered them into a horizontal position on the sea-floor. The stack of white syntactic foam blocks used for buoyancy is clearly visible.

reservoir. This remained as a thin film throughout the experimental period.

The ESWsystem (Fig. S5) was comprised of a 316 stainless steel containment tank with an internal volume of 240 l, an in-line pH sensor to monitor the fluid being delivered to FOCE, a peristaltic pump for metered delivery of the CO_2 enriched sea water, a one-atmosphere electronics housing for pump and valve control, an oil compensated junction box for easy and quick electrical terminations, an oil compensator, and a valve switch box (located on the FOCE frame) for electrically switching the fluid into either end of the flume. It was configured in a trapezoidal cross section (91 cm long, 41 cm tall at one end, 46 cm tall at the other end, and 61 cm wide) resulting in a sloped base. The sloped bottom permits easy withdrawal of the denser ESW from the lower end of the ESW tank.

3.3. *Required quantities of CO_2*

The pH perturbations approximate those predicted from various IPCC emission scenarios (IPCC, 2005) and were adjusted for

the lower buffer capacity of deep sea water. A pH change of −0.3 would be typical for FOCE studies although significantly greater pH stresses can be applied if desired. Given the dimensions of the deployed flume system it was possible to calculate the required quantities of CO_2 for various combinations of flow rate, and background sea water chemistry. In Table 1 we show example calculations in the case of a 0.5 m^2 end face with a 4 cm per s current flow with desired controlled pH shifts of 0.3 and 0.5 pH units below ambient conditions. The mass of sea water moving through a chamber of these dimensions is 1200 kg per min. The energy required for moving this mass of water along a neutral density surface is surprisingly low: only ~120 W is required for the thrusters.

The chemical demands for providing the desired pH shift can then be estimated knowing the background alkalinity and pH of the ocean at this site. The ESW contains a working fluid in near equilibrium with the solubility of CO_2 hydrate. At ambient temperature and pressure the full equilibrium concentration of dissolved CO_2 is 656 mM. Given the small surface area of the interface, and a steady demand for CO_2 ESW, it is unlikely that complete saturation is maintained. For the sake of estimating demand in Table 1, we assumed an ESW CO_2 concentration of 500 mM which is about 75% of saturation. When delivered to the FOCE unit at a rate of about 0.6 l/min this will yield a pH shift of −0.3; while a rate of 1.1 l/min will yield a pH shift of −0.5. Once the ESW tank was filled with liquid CO_2, the contained volume of liquid CO_2 was sufficient to supply the enriched sea water demand for one month with a ΔpH of −0.3 pH units and a 4 cm/s internal flow rate.

3.4. FOCE flume electronics and GUI

A diagram of the FOCE flume hardware, sensors, CO_2-ESW system, and the control system is shown in Figs. S4 and S6. A Linux computer in the main FOCE electronics housing handled control of the various pumps and valves under commands from the FOCE graphical user interface (GUI). The FOCE GUI is a custom designed interface and was written in Java 6. It ran as a stand-alone executable on a Windows laptop. The GUI consisted of a single "window" with seven tabs to select the various data displays: pH, Water Velocity, CTD, Device Control, Environmental Conditions, Power Consumption, and CO_2 Subsystem. Once the operator selected and entered thruster motor speeds, pH calibration offsets, ESW pump speed, etc., the GUI transmitted the appropriate commands via the MARS cable to the FOCE flume on the seafloor. A detailed description of the GUI can be found in the Supporting Information.

The main CPU housing was directly connected to the MARS cabled observatory node via a 30 m underwater mateable ODI cable. This cable carried both power and Ethernet communications. Three power supplies converted the 375 V power from the MARS node to the 12 V, 24 V and 36 V buses within the main housing. This housing also supplied power and communications to the sensors, motors, lights, cameras and pumps.

The ESW electronics housing was mounted on the ESW box and distributed all power and communication to the subsystems via three electrical penetrators. It provided inrush limiting for the 375 VDC input voltage, which was down converted by a 24 VDC Vicor module. 12 VDC and 5 VDC were also generated from the 24 VDC bus for use on lower level subsystems. Power and environmental monitoring were handled through custom built circuit boards. Ethernet-to-serial conversion was handled via a Digi serial server. There was no computer in the ESW subsystem; all control was handled through the main FOCE computer in the main CPU housing.

Table 1
Estimation of the amount of CO_2 enriched seawater working fluid required for three pH shifts at the average background conditions at the FOCE MARS site assuming a 4 cm/s laminar flow velocity inside the FOCE flume.

Cross-sectional area of controlled volume (m^2)		**0.5**	
For a 4 cm/s current			
Volume = area × current velocity (m^3/s)		**0.02**	
Volume = area × current velocity (m^3/min)		**1.2**	
Mass of seawater (kg/min)		**1200**	
pH shift desired	**−0.5**	**−0.3**	**−0.1**
CO_2 required (μmol/kg)	**177.9**	**95.0**	**30.0**
CO_2 required (μmol/min)	**213.5**	**114.0**	**36.0**
ESW CO_2 concentration (mM)	**500**		
Vol ESW required (l/min)	**0.43**	**0.23**	**0.07**
Vol ESW required (l/h)	**26**	**14**	**4**

4. Results

4.1. System testing

Once the system was installed on the sea floor, connected to the MARS node and preliminary command and control functions via the GUI were verified, a series of tests were conducted to investigate the response times and overall stability of the FOCE system. The first of these was a sequence of thruster motor tests to demonstrate the ability to move water through the flume. It was also desired to test if thrusters at both ends of the flume were required or if only one thruster was sufficient to drive the desired flow-rates. In Fig. 6, we show the results of one of these tests. The motor speeds were increased step-wise from 0 to 280 counts then back down to zero and in reverse and back again. Because the thruster motors face opposite directions, the motors had to be operated with opposite signs in order to move water in the same direction. This cycle took 4 h to complete and was repeated 6 times while the interior seawater velocity was monitored using a Vector velocimeter. The motors provided reproducible flow throughout this test.

For the initial pH control test we kept the flow through the flume constant. The result of this test is shown in Fig. 7 (upper panel). We made two additions of CO_2 ESW. The first lasted for 30 min beginning at 15:00 PDT (Pacific Daylight Time), while the second lasted for 90 min beginning at 16:15 PDT. The time offset from when the ESW peristaltic pump was started and when the first pH offset was measured by pH sensors pH3 and pH4 is an indication of the transit time of the seawater to the central chamber inside FOCE. The time lag between the pH offset in the forward pH sensors (pH3 and pH4) and the rear pH sensors (pH1 and pH2) shows the transit time through the central chamber. Since both the forward (pH3 and pH4) and the rear pH sensors (pH1 and pH2) showed a nearly identical pH, the time delay inside the wings was sufficient for almost complete CO_2 equilibration to be achieved. During each addition of ESW, small negative spikes in the external pH (pH5 and pH6) can be seen: one spike between 15:00 and 16:00 PDT, and quite a few between 16:15 and 18:00 PDT. These result from high CO_2 seawater exiting FOCE and being carried back in diluted form across our external pH probes. This reveals the necessity of knowing the external current direction and adjusting the internal flow direction accordingly so that any ESW exiting FOCE will not re-enter the system.

In a second and longer test of the system (Fig. 7, lower panel) we made a single addition of ESW at varying pump speeds to demonstrate that we could select any desired pH offset (within the designed operational limits) via GUI control. The CO_2 ESW pump rate was increased in four steps at 30 min intervals and then

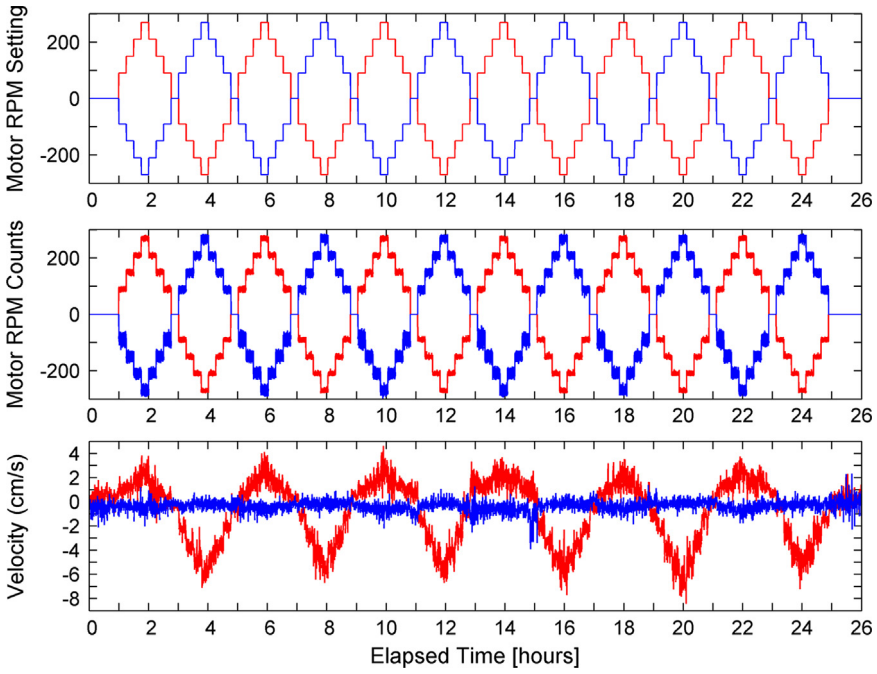

Fig. 6. Upper panel: plot of motor rpm command settings for motor 1 (red) and motor 2 (blue) showing the repeated cycling from 0 rpm/s to +270 then down to zero and to −270 and back to zero. The fan motor speed was controlled by a fan speed 'app' running on the FOCE flume on-board computer. Because the motors are mounted facing in opposite directions, the motors have to turn in opposite directions in order to force the water to move in the same direction. Middle panel: plot of the actual motor rpm/s for motor 1 (red) and motor 2 (blue) as sensed by the on-board control module. Lower panel: plot of internal water velocity (*x*-axis direction/long axis of flume=red; *y*-axis direction/cross axis of flume=blue) as a function of time. Notice that the apparent flow velocity is about three times faster when motor #1 is turning in the negative direction and motor #2 is turning in the positive direction, than when they are turning at the same rpm but with both directions reversed. We were unable to determine whether this was a real effect or strictly the result of a flow sensitivity bias in the Vector velocimeter. (For interpretation of the references to color in this figure legend, the reader is referred to the web version of this article.)

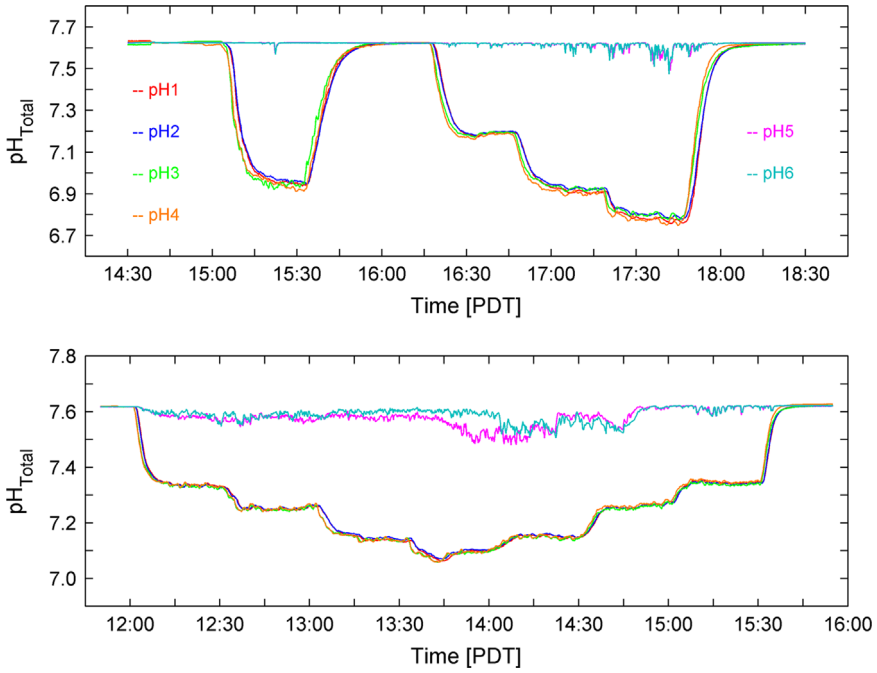

Fig. 7. Upper panel: plot of FOCE flume pH during the first CO_2 ESW trial. There were four pH sensors located inside the flume center section: two forward/upstream (green and yellow traces) and two rear/downstream (red and blue traces). In addition, there were two external pH sensors (magenta and cyan). Two additions of CO_2 ESW were made: the first starting at 15:00 PDT and lasting 30 min at a single addition rate; the second starting at 16:15 PDT and lasting 90 min at varying rates. The lag time between the start of CO_2–ESW pumping and appearance of the low pH seawater in the flume is a measure of the internal water velocity as it transits down the delay wing. Lower panel: plot of FOCE flume pH during the second CO_2 ESW trial. In this trial a single addition of CO_2 ESW was made. As before, the flow of seawater through the plume was held constant while the addition rate of the CO_2 ESW was varied by changing the speed of the peristaltic pump in order to vary the CO_2 mixing ratio and, as a consequence, the seawater pH. Four distinct pump speeds were used to add CO_2 to the chamber and lower the pH; these steps were repeated in reverse to return the CO_2 concentration to background levels and raising the pH. (For interpretation of the references to color in this figure legend, the reader is referred to the web version of this article.)

decreased in four steps again at 30 min intervals. Again the time lag between changes in pump speed and the arrival of the pH shift is clearly seen. Likewise the forward (upstream) pH sensors (pH3 and pH4) record this change before the rear (further downstream) sensors (pH1 and pH2). As all four sensors show nearly identical pH offsets for each of these steps, we concluded that the necessary time for full pH and CO_2 system equilibrium was achieved and that both the pH and CO_2 enrichment levels were uniform within the center chamber where science experiments were to be performed/executed.

4.2. Long term operation

A biological impact experiment lasting 32 days was conducted at the FOCE site (Barry et al., 2014) during which the pH was offset −0.4 to −0.5 from background conditions. Fig. 8 shows physico-chemical data from the first few days of the experiment; this illustrates some of the challenges experienced while running a high CO_2/low pH experiment, in real time remotely in the deep-sea.

Over the course of this 32 day experiment, we were able to manually maintain a pH offset of −0.4 to −0.5 pH units with only minor deviations outside this experimental design specification. Adding real-time pH feedback control of the ESW pump and directional control of the fans according to the ambient sea-floor currents should help to minimize excessive pH excursions in future experiments.

The FOCE flume was continuously deployed at the MARS site for 18 months with 7 pH sensors, 2 CTDs, one Vector velocimeter and one Workhorse ADCP, although the CO_2 releases were carried out only when needed. Data was collected continuously at 1 min intervals from the CTDs and at 10 s intervals from the pH sensors. Over 2 GB of data was collected, not counting the velocimeter or ADCP data. Several minor power interruptions were experienced due to failure of the local utility shore-side power supply. Upon restoration of the power, both the flume and the data collection services re-started automatically. The only mechanical failure we experienced during the 18 month deployment was loss of the chain drive to the motor thrusters at either end of the center chamber due to the unintentional entrainment of animals (hagfish and crabs) in the chains and gear mechanism. During our routine ROV visits to the FOCE site we were able to restore the drive mechanism. The use of a chain guard or a direct drive motor system connected to the thrusters would alleviate this mechanical problem in the future.

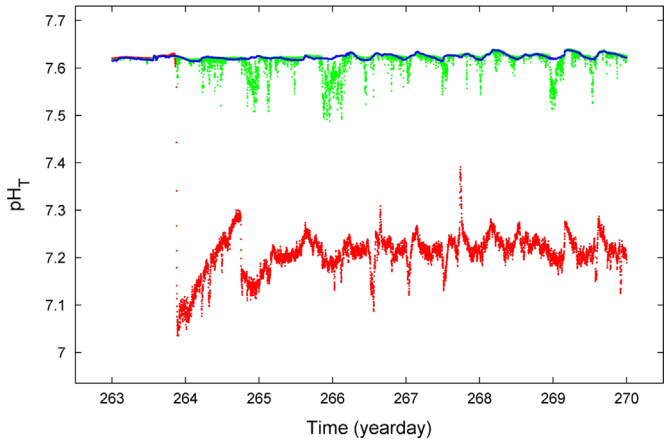

Fig. 8. Plot of pH during the first week of the FOCE biology experiment (Barry et al., 2014) showing the background seawater pH calculated from CTD–O_2 data (blue), the observed exterior pH (green) and the interior pH (red) offset approximately 0.4–0.5 pH units from ambient. The pH fluctuations estimated from CTD data correlate very strongly with our direct pH observations when the system is in background sensing mode with a mean pH of 7.625 and a typical range of ±0.01 pH. The greater range shown by the external pH sensor (green line) here shows local effects of the FOCE system "exhaust" fluids impacting the externally mounted pH sensor. The experiment began with the initiation of CO_2 enrichment late on year day 263 (UTC). After 20 h it was observed that the pH was drifting higher as the fully CO_2 saturated working fluid from the ESW system was being drawn-down and a steady-state CO_2 enrichment was approached. At that time the ESW pump speed was increased and the pH offset was restored. Over the next 24 h a steady-state CO_2 enrichment of seawater was achieved inside the ESW tank and the pH remained relatively constant (except for short periods, see text) for the one month duration of the experiment. (For interpretation of the references to color in this figure legend, the reader is referred to the web version of this article.)

5. Discussion

There is little information on the natural background fluctuations of pH in deep ocean water and thus the time information provided here provides some new insights. The strong auto-correlation of pH with the variance of the controlling species (the CO_2–O_2 system, salinity, and temperature) is well known and we find that the background pH signals at this site were very strongly correlated with CTD data. The dominant local signal we observe is at the tidal frequency with a mean pH_T of 7.625 and daily fluctuations of ±0.01 pH around this mean. Unusual events – benthic storms, mud slides etc. – will undoubtedly occasionally occur with associated short term pH excursions. But the life experience of animals above or at the sediment-water interface at this site is typically confined within a 20–30 milli-pH range on a daily basis and a 50–60 milli-pH range over the course of a year. This stands in sharp contrast to the likely greater change (~0.3 pH) that is predicted from CO_2 emission scenarios. How deep ecosystems adapted to very stable conditions will respond to the combined impacts of changing ocean pH, temperature, and oxygen remains to be seen.

Our experience with this challenging in-situ experimental system was positive, but only after the significant development cycle described here. Subsequent and concurrent to these efforts a number of shallow water FOCE systems have been rapidly developed (Kline et al., 2012; Gattuso et al., 2014), and used for biological studies (Barry et al., 2014). These new systems and experiments draw upon the chemical, physical, and engineering FOCE principles pioneered here. For further information on the continuing development of this field, please see the xFOCE website (http://www.xfoce.org/).

Use of this system need not be limited to FOCE experiments only. With the addition of a heater to the seawater inlet wings, CO_2 enrichment and global warming impacts can be studied either individually or simultaneously. Likewise, the impact of lower oxygen levels can be studied by adding a suitable amount of sodium sulfite to reduce the oxygen concentration in the seawater feed (Wong and Zhang, 1992). Given that none of these effects happens in isolation, the ability to study their impacts simultaneously would be most advantageous.

Acknowledgements

This work was supported by a grant to the Monterey Bay Aquarium Research Institute from the David and Lucile Packard Foundation. We relied upon the critical infrastructure provided by the MARS cable system supported by NSF Grant OCE-1114794. We thank the captains and crew of the RV Point Lobos and RV Western Flyer, and the skilled pilots of the ROVs Ventana and Doc Ricketts who made deployment and operation of this complex system possible.

Appendix A. Supporting information

Supplementary data associated with this article can be found in the online version at http://dx.doi.org/10.1016/j.dsr.2014.11.005.

References

Barry, J.P., Buck, K.R., Lovera, C.F., Kuhnz, L., Whaling, P.J., Peltzer, E.T., Walz, P.M., Brewer, P.G., 2004. Effects of direct ocean CO_2 injection on deep-sea meiofauna. J. Oceanogr. 60, 759–766.

Barry, J.P., Buck, K.R., Lovera, C., Kuhnz, L, Whaling, P.J., 2005. Utility of deep-sea CO_2 release experiments in understanding the biology of a high CO_2 ocean: effects of hypercapnia on deep-sea meiofauna. J. Geophys. Res. Oceans 110, C09S12.

Barry, J.P., Lovera, C., Buck, K.R., Peltzer, E.T., Taylor, J.R., Walz, P.M., Whaling, P.J., Brewer, P.G., 2014. Use of a Free Ocean CO_2 Enrichment (FOCE) system to evaluate the effects of ocean acidification on the foraging behavior of a deep-sea urchin. Environ. Sci. Technol. 48 (16), 9890–9897. http://dx.doi.org/10.1021/es501603r.

Brewer, P.G., Bradshaw, A., 1975. The effect of non-ideal composition of seawater on salinity and density. J. Mar. Res. 33, 157–175.

Brewer, P.G., Friederich, G., Peltzer, E.T., Orr Jr., F.M., 1999. Direct experiments on the ocean disposal of fossil fuel CO_2. Science 284, 943–945.

Brewer, P.G., Peltzer, E.T., Walz, P.M., Aya, I., Yamane, K., Kojima, R., Nakajima, Y., Nakayama, N., Haugan, P., Johannessen, T., 2005. Deep ocean experiments with fossil fuel carbon dioxide: creation and sensing of a controlled plume at 4 km depth. J. Mar. Res. 63, 9–33.

Brewer, P.G., 2013. A short history of ocean acidification science in the 20th century: a chemist's view. Biogeosciences. http://dx.doi.org/10.5194/bgd-10-1-2013.

Cicerone, R., Orr, J., Brewer, P.G., Haugan, P., Merlivat, L., Ohsumi, T., Pantoja, S., Poertner, H.O., 2004. The ocean in a high CO_2 world. Eos Trans. AGU 85, 351–353.

DeLucia, E.H., J.G., Hamilton, J.G., Naidu, S.L., Thomas, R.B., Andrews, J.A., Finzi, A., Lavine, M., Matalama, R., Mohan, J.E., Hendrey, G.R., Schlesinger, W.H., 1999. Net primary production of a forest ecosystem with experimental CO_2 enrichment. Science 284, 1177–1179.

Dunk, R.M., Peltzer, E.T., Walz, P.M., Brewer, P.G., 2005. Seeing a deep ocean CO_2 enrichment experiment in a new light: laser Raman detection of dissolved CO_2 in seawater. Environ. Sci. Technol. 39, 9630–9636.

Favali, P., Beranzoli, L., 2006. Seafloor observatory science: a review. Ann. Geophys 49, 515–567.

Favali, P., Person, R., Barnes, C.R., Kaneda, Y., Delaney, J.R., Hsu, S.-K. 2010. Seafloor observatory science. In: Hall, J., Harrison, D.E., Stammer D. (Eds.), Proceedings of the OceanObs'09: Sustained Ocean. Observations and Information for Society Conference 2, Venice, Italy, 21–25 September 2009, ESA Publication WPP-306, ISSN:1609-042X, http://dx.doi.org/10.5270/OceanObs09.cwp28.

Gattuso, J.-P., Kirkwood, W., Barry, J., Cox, E., Gazeau, F., Hansson, L., Hendriks, I., Kline, D., Mahacek, P., Martin, S., McElhany, P., Peltzer, E.T., Reeve, J., Roberts, D., Saderne, V., Widdicombe, S., Brewer, P.G., 2014. Free ocean CO_2 enrichment (FOCE) systems: present status and future developments. Biogeosciences 11, 4001–4046. http://dx.doi.org/10.5194/bgd-11-4001-2014.

IPCC, 2005. Carbon Dioxide Capture and Storage (Special Report of WG III). Cambridge University Press p. 431.

Johnson, K.S., 1982. Carbon dioxide hydration and dehydration kinetics in sea water. Limnol. Oceanogr. 27 (849-845).

Kline, D.I., Teneva, L., Schneider, K., Miard, T., Chai, A., Marker, M., Headley, K., Opdyke, B., Nash, M, Valetich, M., Caves, J.K., Russell, B., Connell, S., Kirkwood, W., Brewer, P., Peltzer, E., Silverman, J., Caldeira, K., Dunbar, R.B., Koseff, J.R., Monismith, S.G., Mitchell, B.G., Dove, S., Hoegh-Guldberg, O., 2012. A short-term in situ CO_2 enrichment experiment on Heron Island (GBR). Sci. Rep 2, 413. http://dx.doi.org/10.1038/srep00413.

Long, S.P., Ainsworth, E.A., Leakey, A.B., Nosberger, J., Ort, D.R., 2006. Food for thought: lower-than-expected crop yield stimulation with rising CO_2 concentrations. Science 312, 1918–1921.

Marchetti, C., 1977. On geoengineering the CO_2 problem. Clim. Change 1, 59–68.

Massion, E., Raybould, K., 2006. MARS, the Monterey accelerated research system. Sea Technol. 47, 39–42.

Nakayama, N., Peltzer, E.T., Walz, P., Brewer, P.G., 2005. First results from a controlled deep-sea CO_2 perturbation experiment: evidence for rapid equilibration of the oceanic CO_2 system at depth. J. Geophys. Res. 110, C09S11. http://dx.doi.org/10.1029/2004JC002597.

PCAST (President's Council of Advisors on Science and Technology), 1997. Federal Energy Research and Development Agenda for the Challenges of the Twenty-First Century. US Dept. of Energy, Washington, DC (November).

Shaw, H.R., Zavaleta, E.S., Chiariello, N.R., Cleland, E.L., Mooney, H.A., Field, C.B., 2002. Grassland responses to global environmental changes suppressed by elevated CO_2. Science 298, 1987–1990.

Special section: advances in biological research for CO_2 ocean sequestration. In: Shirayama, Y., Kogure, K. (Eds.), J. Oceanogr., 60; 2004, pp. 691–816.

Soli, A.L., Byrne, R.H., 2002. CO_2 system hydration and dehydration kinetics and the equilibrium CO_2/H_2CO_3 ratio in aqueous NaCl solution. Mar. Chem. 78, 65–73.

Tamburri, M., Peltzer, E.T., Friederich, G., Aya, I., Yamane, K., Brewer, P.G., 2000. A field study of the effects of CO_2 disposal on mobile deep-sea animals. Mar. Chem. 72, 95–101.

Thistle, D., Sedlacek, L, Carman, K.R., Fleeger, J.W., Brewer, P.G., Barry, J.P., 2006. Simulated sequestration of industrial carbon dioxide at a deep-sea site: effects on harpacticoid-copepod species. J. Exp. Mar. Biol. Ecol. 330, 151–158.

Thistle, D., Sedlacek, L., Carman, K.R., Fleeger, J.W., Brewer, P.G., Barry, J.P., 2007. Exposure to carbon dioxide-rich seawater is stressful for some deep-sea species: an in situ, behavioral study. Mar. Ecol. Progr. Ser. 340, 9–16.

Widdicombe, S., Blackford, J.C., Spicer, J.I., 2013. Assessing the environmental consequences of CO_2 leakage from geological CCS: generating evidence to support environmental risk assessment. Mar. Pollut. Bull., 399–401.

Wong, G.T.F., Zhang, L-S., 1992. Chemical removal of oxygen with sulfite for the polarographic or voltammetric determination of iodate and iodide in seawater. Mar. Chem. 38, 109–116.

Zeebe, R.E., Wolf-Gladrow, D.A., Jansen, H., 1999. On the time required to establish chemical and isotopic equilibrium in the carbon dioxide system in sea water. Mar. Chem. 65, 135–153.

Zeebe, R.E., Wolf-Gladrow, D.A., 2001. CO_2 in Seawater: Equilibrium, Kinetics, Isotopes, no. 65 in Elsevier Oceanography Series, first ed. Elsevier.